J Electr Eng Technol.2018; 13(6): 2178-2186
http://doi.org/10.5370/JEET.2018.13.6.2178

ISSN(Print) 1975-0102
ISSN(Online) 2093-7423

A Load Identification Method for ICPT System Utilizing Harmonics

Chen-Yang Xia†, Wen-Ting Zhu*, Nian Ma*, Ren-Hai Jia* and Qiang Yu*

Abstract – Online identification of load parameters is the premise of establishing a stable and highly-efficient ICPT (Inductive Coupled Power Transfer) system. However, compared with pure resistive load, precise identification of composite load, such as resistor-inductance load and resistance-capacitance load, is more difficult. This paper proposes a method for detecting the composite load parameters of ICPT system utilizing harmonics. In this system, the fundamental and harmonic wave channel are connected to the high frequency inverter jointly. The load parameter values can be obtained by setting the load equation based on the induced voltage of secondary-side network, the fundamental wave current, as well as the third harmonic current effective value received by the secondary-side current via Fourier decomposition. This method can achieve precise identification of all kinds of load types without interfering the normal energy transmission and it can not only increase the output power, but also obtain higher efficiency compared with the fundamental wave channel alone. The experimental results with the full-bridge LCCL-S type voltage-fed ICPT system have shown that this method is accurate and reliable.

Keywords: Composite load, Double channel, Fourier decomposition, Harmonics, Identification, Inductive coupled power transfer.

1. Introduction

ICPT technology as a wireless power transfer approach from power source to terminal using spatial electro-magnetic fields, not only overcomes the disadvantages of traditional power supply mode, but also is of high safety and reliability and easy to fix and maintain, thus receiving a lot of concern from experts at home and abroad. At present, this technology has been widely applied in many specific fields like electric vehicle [1], mobile phones [2], household appliances [3], coal mining [4], underwater [5], built-in device of human powered externally [6] and so on.

As we all know, ICPT system is a high-order nonlinear and parameter sensitive system whose primary and secondary sides separate physically. Any possible change will influence the power transmission characteristics, even cause faults in the system, particularly with parameter variation of the secondary side such as load properties and measure. Therefore, it is necessary to detect and apperceive the load in real time to adjust circuit condition by effective controlling strategy to ensure stability and high-efficient operation of the circuit.

In the past, there are many researches of pure resistive load at home and abroad [7-12], but few with regard to the composite load like resistor-inductance [13-17] and resistance-capacitance. A method of load identification which focuses on the PS-type based on the least square method is proposed, but the algorithm is relatively complicated [7]; According to differential equations of the primary winding current envelop under full resonant mode, the resistive load value is achieved. However, the energy source has been cut off in the load identifying process [8,9]; In addition, the load parameters can be detected according to the muti-winding magnetic circuit structure and induced voltage [10]; The resistive load value is calculated based on genetic algorithm and input voltage and current [11].

However, there are many problems in load identification technologies: the calculation or control process is relatively complicated; Nor normal wireless transmission can be ensured in the process of load identification, etc. Therefore, this paper raises a method to identify load parameters of ICPT system utilizing harmonics. In this system, the fundamental and harmonic wave channel are connected to the high frequency inverter jointly. And the load parameter value can be obtained by setting the load equations based on induced voltage of secondary-side network, the fundamental current as well as the third harmonic current effective value received by the secondary-side current via Fourier decomposition. This technology can not only achieve precise online identification of all kinds of load types without interfering normal power transmission and it can not only increase the output power, but also increase system transmission power when entering into harmonic channel. The experiment indicates that it is reliable and applicable to achieve the load identification utilizing harmonics.

† Corresponding Author: School of Electrical and Power Engineering, China University of Mining and Technology, Xuzhou, China. (18260722082@163.com)
* China University of Mining and Technology, Xuzhou, China. (15052008952@163.com, 1597605432@qq.com, jiarenhai@cumt.edu.cn, yuqiang1008hotmail.com)
Received: March 14, 2018; Accepted: June 19, 2018

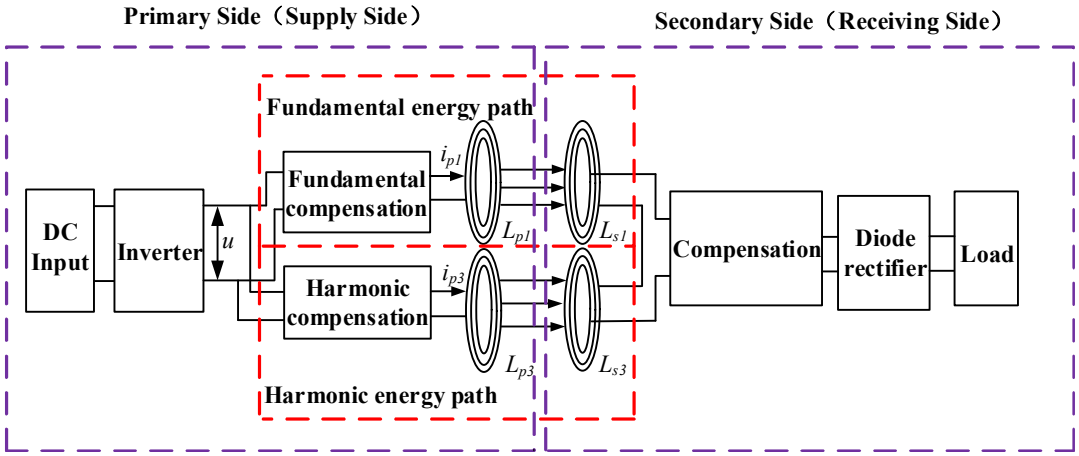

Fig. 1. Work block diagram of ICPT system utilizing harmonics

2. Principle Analysis of Load Identification of ICPT Utilizing Harmonics

The fundamental-harmonic double channel inductive coupled power transmission system is composed of DC input, inverter and its driving circuit, fundamental and harmonic compensation networks, magnetic circuit mechanism, diode rectifier and load, which is showed in Fig. 1.

In this system, the fundamental and harmonic wave channel are connected to the high frequency inverter jointly. Parameters of the primary and secondary-side resonance compensating network is first set out, followed by establishment of the fundamental wave and harmonics transmission channel respectively. Then the real-time transmission of power of the double channel can be achieved. The working mode can effectively improve the system's voltage adjustment range and efficiency [18]. In order to analyze the principle of the online load identification, system parameters are reported as follows:

(1) The primary section of the fundamental channel achieves full resonance under fundamental frequency, i.e., the working frequency of inverter switching devices;

(2) The primary section of the harmonic channel achieves full resonance under harmonic frequency;

(3) The secondary-side network contains pick-up coils from the double channels and the compensation capacitor. And it is designed for full resonance under fundamental frequency;

(4) The fundamental and harmonics transmission coils are devised to work at the output constant current mode to ensure induced voltage of the secondary-side network constant with the load change;

(5) According to magnetic circuit structure design, mutual inductance between primary transmitting coils and the secondary-side pick-up coils of the double channel is considered ignoring the cross-coupling.

Since the third harmonic content of the rectangular

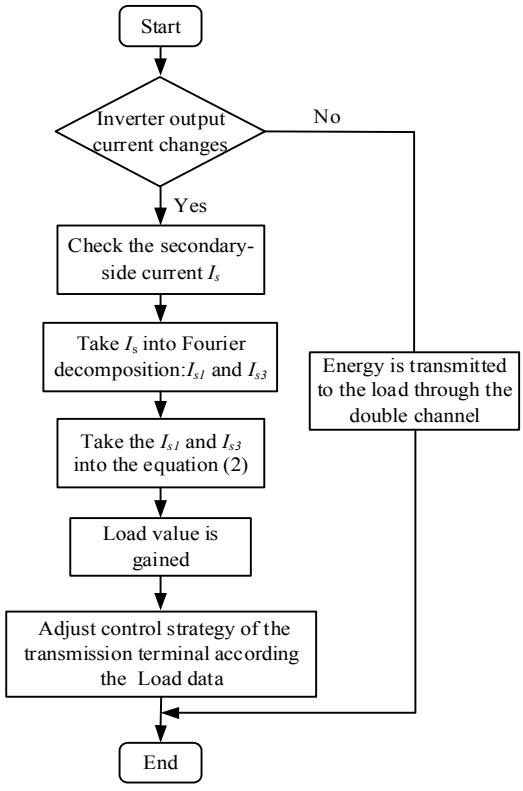

Fig. 2. Work flow chart of load identification

voltage generated by inverter is just lower than the fundamental. Thus, this paper takes the example of establishing the third harmonic channel, the working principle of load identification is showed in Fig. 2, that is: waveform and value of inverter output current are inspected at all times which changes with loads because the inverter output voltage is constant. Therefore, we can find out whether the system loads change through current detection; if the current keeps constant, energy is transmitted to the load through the fundamental-harmonic double channel; to the contrary, the system loads needs identified. Both fundamental and third harmonic will work

on the secondary-side network at the same time. Thus, the induced voltage us on the secondary-side circuit is the superposition of a couple of frequency-voltages, which is defined based on the following equation:

$$\begin{cases} u_{s1} = \sqrt{2}U_{s1}\cos(\omega t) = \sqrt{2}\omega M_1 I_{p1}\cos(\omega t) \\ u_{s3} = \sqrt{2}U_{s3}\cos(3\omega t) = 3\sqrt{2}\omega M_3 I_{p3}\cos(3\omega t) \\ u_s = u_{s1} + u_{s3} \end{cases} \quad (1)$$

Where ω is the working frequency of the inverter. u_{s1} and u_{s3} are the induced voltage values of the fundamental wave channel and the third harmonic channel respectively. M_1 and M_3 are mutual inductances of the fundamental wave coupling structure and the third harmonic coupling structure respectively. I_{p1} and I_{p3} are the transmitting coil current effective values of the fundamental wave channel and the third harmonic channel respectively. The secondary circuit current reflects joint performance of fundamental and the third harmonic. So the secondary-side current i_s is checked firstly and then the fundamental wave current I_{s1} and the third harmonic wave current I_{s3} can be obtained by taking is into Fourier decomposition. According to superposition theorem and relationship between load voltage and current, the equation of load parameters can be formulated. Taking the resistor-inductance load (resistance R, inductance L) as an example, Eq. (2) can be written as follows.

$$\begin{cases} \dfrac{\omega M_1 I_{p1}}{\sqrt{R^2 + (\omega L)^2}} = I_{s1} \\ \dfrac{3\omega M_3 I_{p3}}{\sqrt{R^2 + (X + 3\omega L)^2}} = I_{s3} \end{cases} \quad (2)$$

Since the secondary-side network can achieve full resonance under the fundamental frequency, the X in (2) is the impedance value in the system secondary-side network except resistor-inductance load under the third harmonic frequency.

Above all, load value is gained by solving (2). After load identification, the load parameters are transmitted to the primary side through signal transmission circuit. Then the primary energy emission mechanism can adjust control strategy of the transmission terminal according to feedback data, and thus enables real-time tracking of system power and efficiency. At this time, it does not cut off the energy transmission in the process of load recognition which is one of the advantages and this method also applies to RC load.

3. Analysis of ICPT System Topology Selection

According to (2), the key point to load identification utilizing harmonics is about the size of the induced voltage u_s performed on the secondary circuit and the load current i_s. When system working frequency and mutual inductance parameters are fixed, identification procedure will be largely simplified if the secondary-side induced voltage produced by the primary current keep constant with the load change. The compensation topology LCL and LCCL both can keep the primary current constant if the requirements are met [19]. However, the method proposed in the paper not only need to keep the primary current constant, but also possess better frequency selection characteristics. Therefore, comparative analysis of LCL and LCCL is necessary to determine the final system compensation topology.

3.1 Analysis of the constant current characteristics of the primary side

Fig. 3 is the LCL and LCCL reactive compensation topologies.

U is the voltage source; L_{a1} and L_{a2} are the primary coils; C_{p1} and C_{p2} are the compensation capacitances; C is the primary capacitance; L_{p1} and L_{p2} are the transmission coils; Z_R is the load; $Z_{in\text{-}LCL}$ and $Z_{in\text{-}LCCL}$ are the total impedance seen from U; Z_a and Z_b are the equivalent impedance seen from the compensation capacitances C_{p1} and C_{p2} respectively. According to paper [18-19], if the parameter in Fig. 3 can be written as:

$$\begin{cases} L_{a1} = L_{p1} \\ j\omega L_{a2} = j\omega L_{p2} + \dfrac{1}{j\omega C} \end{cases} \quad (3)$$

The primary current $I_{L\text{-}LCL}$, $I_{L\text{-}LCCL}$ are fixed values as follows:

$$\begin{cases} \dot{I}_{L\text{-}LCL} = \dfrac{\dot{U}}{j\omega L_{a1}} \\ \dot{I}_{L\text{-}LCCL} = \dfrac{\dot{U}}{j\omega L_{a2}} \end{cases} \quad (4)$$

Therefore, LCL and LCCL topology both are able to keep the primary current constant.

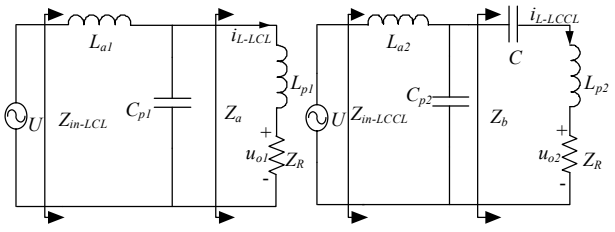

(a) LCL Topology (b) LCCL Topology

Fig. 3. The LCL and LCCL reactive compensation topology

3.2Analysis of frequency selection characteristics

The Harmonic Ratio of I_n, i.e., HRI_n, is the technical index to measure the system frequency selection characteristics. And the method proposed in this paper needs to select the third harmonic from the voltage square waves accurately. In order to improve the frequency selection characteristics of the primary resonance network, it's necessary to analyze whose frequency selection characteristics is better.

According to Fig. 3, the total impedance $Z_{in}(n\omega)$ of the n-th harmonic are

$$\begin{cases} Z_{in\text{-}LCL}(n\omega) = jn\omega L_{a1} + \dfrac{1}{jn\omega C_{p1}} // Z_a \\ Z_{in\text{-}LCCL}(n\omega) = jn\omega L_{a2} + \dfrac{1}{jn\omega C_{p2}} // Z_b \end{cases} \tag{5}$$

Then the primary current equation can be written as follows:

$$\begin{cases} \dot{I}_{Ln\text{-}LCL} = \dfrac{\dot{U}/n}{Z_{in\text{-}LCL}(n\omega)} \times \dfrac{\dfrac{1}{jn\omega C_{p1}}}{\dfrac{1}{jn\omega C_{p1}} + Z_a} \\ \dot{I}_{Ln\text{-}LCCL} = \dfrac{\dot{U}/n}{Z_{in\text{-}LCCL}(n\omega)} \times \dfrac{\dfrac{1}{jn\omega C_{p2}}}{\dfrac{1}{jn\omega C_{p2}} + Z_b} \end{cases} \tag{6}$$

From the analysis above, the HRI_3 of LCL and LCCL topology can be obtained as bellows:

Table 1. Parameter design of LCL/LCCL reactive compensation topology

Parameters	Values	Parameters	Values
U/V	60	f/Hz	20k
L_{a1}/μH	134.7	L_{a2}/μH	134.7
C_{p1}/μF	0.47	C_{p2}/μF	0.47
L_{p1}/μH	134.7	L_{p2}/μH	198
C/μF	1		

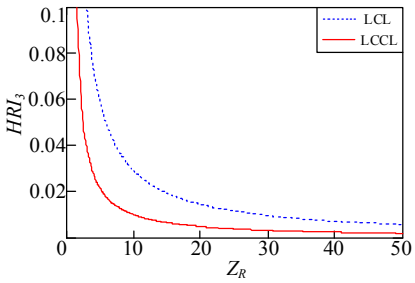

Fig. 4. The change rule of $HRI_{3\text{-}LCL}$ and $HRI_{3\text{-}LCCL}$ with the variation of load resistance Z_R

$$\begin{cases} HRI_{3-LCL} = \left| \dfrac{\dot{I}_{L3-LCL}}{\dot{I}_{L1-LCL}} \right| \\ HRI_{3-LCCL} = \left| \dfrac{\dot{I}_{L3-LCCL}}{\dot{I}_{L1-LCCL}} \right| \end{cases} \tag{7}$$

In order to compare the frequency selection characteristics of LCL and LCCL topology, the change curves of $HRI_{3\text{-}LCL}$ and $HRI_{3\text{-}LCCL}$ with the load are shown in Fig. 4 according to the actual parameters shown in Table 1.

On the basis of Fig. 4, under the same load resistance, the harmonic ratio for I_3 of LCCL topology is lower, therefore the frequency selection is better. In a word, LCCL compensation topology is not only able to keep the primary current constant, but also solves the interaction problem of parameter selection in LCL. Meanwhile, since the secondary circuit needs constant voltage while the series resonance can largely reduce the system complexity if requirements are met. Therefore, this paper chooses LCCL-S as the resonance network topology of this system which is shown in Fig. 5.

In Fig. 5, U_d is input DC voltage source; G_1−G_4 are the power MOSFET, which comprises the full inverter. The fundamental energy path consists of the primary fundamental wave coil L_{a1}, the compensation capacitance C_{p1}, the fundamental wave capacitance C_1, the fundamental transmission coil L_{p1} and its internal resistance R_{p1} and secondary-side fundamental wave pick-up coil L_{s1}. The harmonic energy path is composed of the primary harmonic coil L_{a3}, the compensation capacitance C_{p3}, the harmonic capacitance C_3, the harmonic transmission coil L_{p3} and its internal resistance R_{p3}, and secondary-side harmonic wave pick-up coil L_{s3}. The system secondary-side network is made up of the fundamental-harmonic pick-up coils L_{s1} and L_{s3}, compensation capacitance C_s and the load Z (R, L) which remains to be identified.

4. Analysis of the System Power and Efficiency Characteristics

According to the ICPT system for load identification utilizing harmonics shown in Fig. 5 and analysis in the first chapter, induced voltage us overlaps the fundamental and third harmonic. The secondary-side network induced voltage is

$$u_s = \sqrt{2}\omega M_1 I_{p1} \cos\omega t + 3\sqrt{2}\omega M_3 I_{p3} \cos 3\omega t \tag{8}$$

In a non-sinusoidal periodic circuit, the system average power is the algebraic sum of the power made up of constant component and average power of each harmonic. On the basis of the system composition and the secondary-side induced voltage formula, taking the resistor-inductance load Z(R, L) as an example, the power

expression can be achieved as

when n=1

$$\dot{I}_{s1}=\frac{U_{s1}\angle 0°}{R+j\omega L}=\frac{U_1M_1}{L_{a1}\sqrt{R^2+(\omega L)^2}}\angle-\alpha \tag{9}$$

$$P_1=\left|\dot{I}_{s1}\right|^2R=\frac{U_1^2M_1^2R}{L_{a1}^2\left(R^2+\omega^2L^2\right)} \tag{10}$$

when n=3

$$\dot{I}_{s3}=\frac{U_{s3}\angle 0°}{R+j(3\omega L+X)}=\frac{U_3M_3}{L_{a3}\sqrt{R^2+(3\omega L+X)^2}}\angle-\beta \tag{11}$$

$$P_3=\left|\dot{I}_{s3}\right|^2R=\frac{U_3^2M_3^2R}{L_{a3}^2\left(R^2+(3\omega L+X)^2\right)} \tag{12}$$

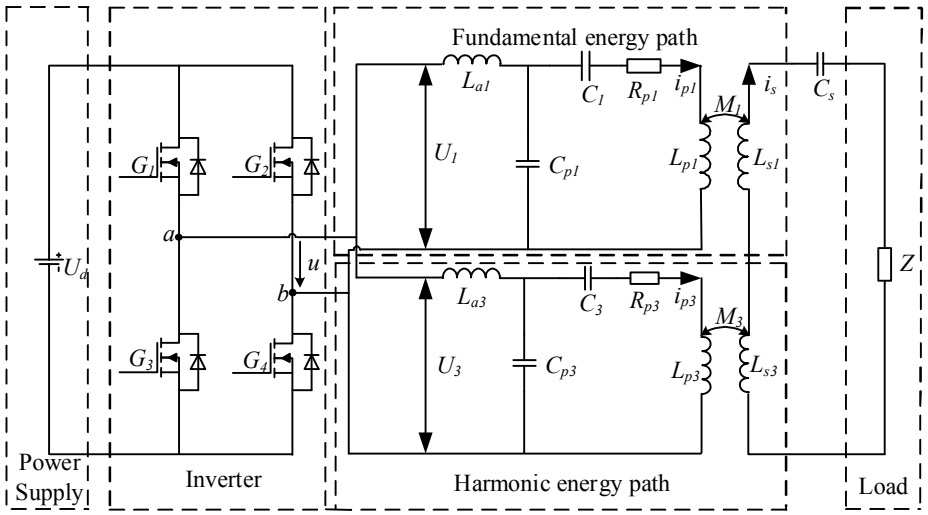

Fig. 5. ICPT system for load identification utilizing harmonics

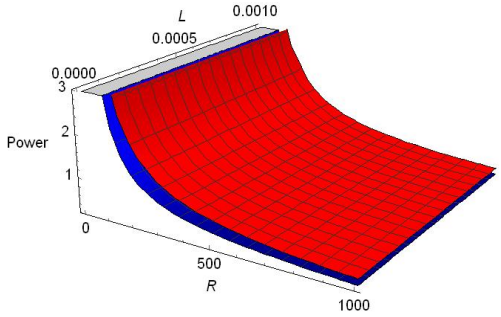

(a) The output power variation curve with load size

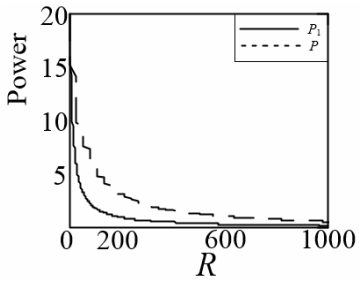

(b) The variation curve of power with load resistance under a certain inductance

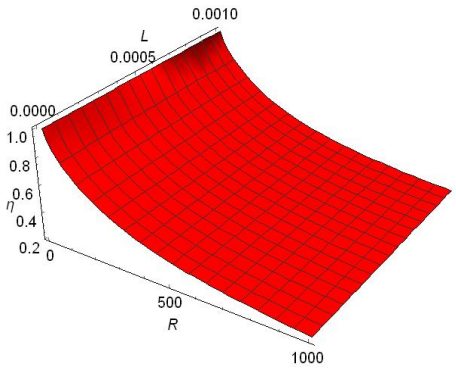

(c) The system efficiency variation curve with load size

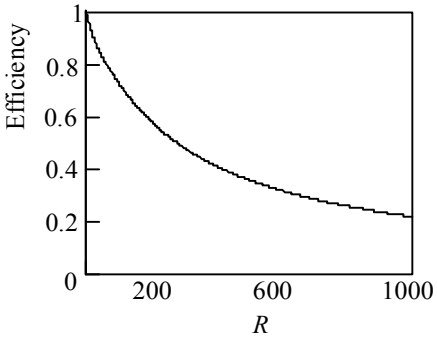

(d) The variation curve of system efficiency with load resistance under a certain inductance

Fig. 6. System output power and efficiency variation curve with load

where $\tan\alpha = \dfrac{\omega L}{R}, \tan\beta = \dfrac{3\omega(3\omega L + X)}{R}$

According to Fig. 5, the inverter output voltage U_1 of the fundamental wave channel, U_3 of the harmonic channel and the X value in (2) are:

$$\begin{cases} U_1 = \dfrac{2\sqrt{2}U_d}{\pi} \\ U_3 = \dfrac{2\sqrt{2}U_d}{3\pi} \end{cases} \quad X = 3\omega(L_{s1} + L_{s3}) - \frac{1}{3\omega C_s} \tag{13}$$

Therefore, when fundamental and harmonics have the combined performance on the secondary-side network, the system output power and efficiency are

$$P_{out} = P_1 + P_3 = \left|\dot{I}_{s1}\right|^2 R + \left|\dot{I}_{s3}\right|^2 R \tag{14}$$

$$\eta = \frac{\left|\dot{I}_{s1}\right|^2 R + \left|\dot{I}_{s3}\right|^2 R}{\left|\dot{I}_{s1}\right|^2 R + \left|\dot{I}_{s3}\right|^2 R + \left(\dfrac{U_1}{\omega L_{a1}}\right)^2 R_{p1} + \left(\dfrac{U_3}{3\omega L_{a3}}\right)^2 R_{p3}} \tag{15}$$

With the change of load, the varying curve between the output power and efficiency and the load is shown in Fig. 6. Among them, the (a) and (b) describe the relationship between the output power and load, the solid line expresses the double channel while the solid line indicates the fundamental wave in (b). It can be seen from the figure, the double channel ICPT system receives more output power compared with the fundamental wave channel. The (c) and (d) show the curves of the system efficiency changing with the load and the efficiency is not effected by the inductive part nearly. From the former analysis and the curve, it can be concluded that the system obtains higher efficiency under heavy load condition and lower efficiency under light load condition.

The system has the characteristics of constant primary current and the constant secondary-side voltage, thus has higher efficiency under heavy load, and lower efficiency under light load, which can be also seen from the previous figure. Furthermore, coil inner resistance and cross coupling in the magnetic circuit coupling structure also influence efficiency. Therefore, such factors should be taken into consideration when designing the system parameters and magnetic circuit structure.

5. Design of Magnetic Circuit Structure

According to the previous analysis, this system has two magnetic circuit structures. Among these, the mutual inductance M_1 between the primary transmission coil L_{p1} and the secondary-side pick-up coil L_{s1} in the fundamental wave channel, the mutual inductance M_3 between the primary transmission coil L_{p3} and the secondary-side pick-up coil L_{s3} in the harmonic wave channel are used effectively ignoring the cross coupling.

The premise of this technology is that there is no cross coupling between the magnetic circuit structures. Thus, it's necessary to adjust this system magnetic circuit structure to reduce cross coupling interference among each coil.

According to Fig. 5, there are four inductances L_{p1}, L_{s1}, L_{p3}, and L_{s3} in the main circuit topology with the fundamental-harmonic double channel. Theoretically, there are six mutual inductances. In order to ignore the other four cross coupling mutual inductances, this paper designs the electromagnetic coupling structure shown in Fig. 7. This magnetic structure consists of the double U-shaped mode magnetic circuit structure whose primary shape and secondary-side shape are completely symmetric orthogonal. Taking the primary structure as an example: two groups of coils are respectively wound on the arms of the U type magnetic circuit mechanism and are connected in series to make up the primary coil of the fundamental wave channel. And two groups of coils are respectively arranged on the two arms of an orthogonal U type magnetic circuit mechanism then are connected in series to make up the primary coil of the harmonic channel. The secondary-side orthogonal magnetic circuit structure is the same with the primary one, the platform of this structure is shown in Fig. 7(a). The primary coil of the fundamental-harmonic channel is vertical to the secondary-side coil respectively, thus forming an orthogonal magnetic circuit structure shown in Fig. 7(b).

The experimental model based on Fig. 7 is constructed, and it is revealed that the self-induction of the primary coil and the secondary-side coil is 231μH, and the distance between the primary and secondary coil of the fundamental-harmonic channel is 40mm. Each inductance value of the electromagnetic circuit coupling structure is shown in Table 2 through measurement.

According to Table 2, the mutual inductance value in

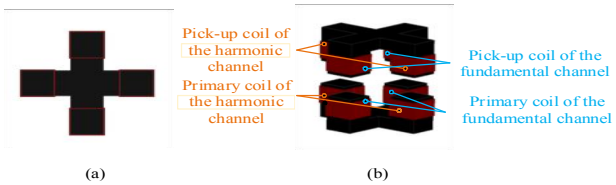

Fig. 7. The structure of the magnetic circuit: (a) Planform magnetic circuit mechanism; (b) Front Elevation of magnetic circuit mechanism

Table 2. Self and mutual inductances of the double U-shaped magnetic circuit structure

M/μH	L_{p1}/μH	L_{s1}/μH	L_{p3}/μH	L_{s3}/μH
L_{p1}/μH	231.5	95.5	0.03	0.01
L_{s1}/μH	95.5	231.5	0.008	0.04
L_{p3}/μH	0.03	0.008	231.5	95.5
L_{s3}/μH	0.01	0.04	95.5	231.5

this magnetic circuit structure is several thousand times of the cross coupling mutual inductance. Therefore, the cross coupling can be ignored, and the magnetic circuit structure can basically meet the requirements of the design in this paper.

6. Experimental Verification

Experimental platform is established in Fig. 8 with the switching frequency is 20kHz based on the system structure diagram in Fig. 5.

Firstly, this paper analyzes the primary coil current of the fundamental-harmonic channel; Secondly, constant current and frequency-selection characteristics are verified; Thirdly, different loads based on system parameters given in Table 3 are identified, and the experiment results of the load identification are shown in Table 4 and Fig. 10, and the Z_1~Z_8 are loads to be identified. According to the experiment, the primary coil inner resistances of the fundamental-harmonic channel are R_{p1}=0.05Ω, R_{p3}=0.02Ω. The secondary-side induced voltage can be calculated as U_{s1}=15.54V, U_{s3}=11.82V, X=45.15 on the basis of the data in the table 3 and Eq. (1), (14).

Fig. 9 is the experimental waveform of a certain load: R=50Ω, L=100μH. According to Fig. 9 (a), (b), (c), it can be seen that the frequency selection characteristic of LCCL topology is relatively better than LCL. The primary coil current value doesn't change when the load parameters change, indicating the constant current characteristic of LCCL compensation topology. Fig. 9(d) is the secondary-

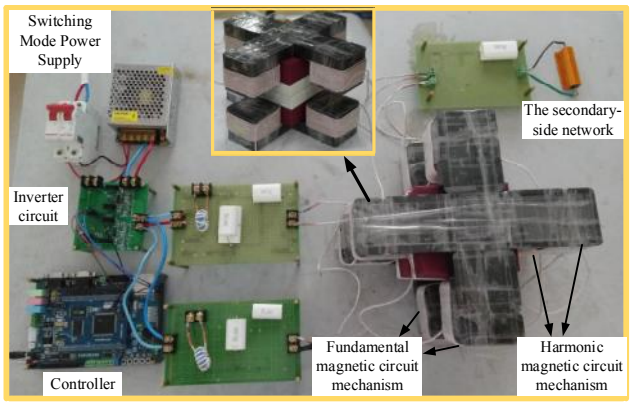

Fig. 8. Hardware experimental platform

Table 3. Parameters of ICPT system for load identification utilizing harmonics

Parameters	Values	Parameters	Values
U_d/V	25	C_s/μF	0.47
L_{a1}/μH	40.33	L_{a3}/μH	4.482
C_{p1}/μF	1.57	C_{p3}/μF	1.57
C_1/μF	0.4702	C_3/μF	0.1012
L_{p1}/μH	175	L_{p3}/μH	74
L_{s1}/μH	67.37	L_{s3}/μH	67.37

Table 4. Experiment results of the load identification

Load condition	Experiment Results	Accuracy		Efficiency
		Real part	Imaginary part	
R=10Ω L=50μH	R=10.6Ω L=48.1μH	94%	96.2%	91.2%
R=10Ω L=100μH	R=10.5Ω L=96.3μH	95%	96.3%	90.3%
R=20Ω L=50μH	R=20.6Ω L=48.8μH	97%	97.6%	88.6%
R=20Ω L=100μH	R=20.8Ω L=96.3μH	96%	96.3%	88.1%
R=50Ω L=100μH	R=48.95Ω L=97.4μH	97.9%	97.4%	85.2%
R=50Ω L=200μH	R=49.1Ω L=197.8μH	98.2%	98.9%	84.9%
R=100Ω L=100μH	R=100.4Ω L=92.8μH	99.6%	92.8%	79.8%
R=100Ω L=200μH	R=100.4Ω L=195.4μH	99.6%	97.7%	78.3%

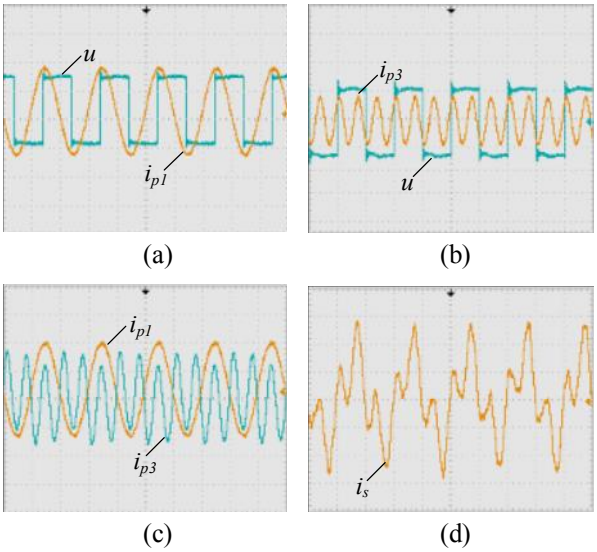

Fig. 9. Experimental waveform of the system: (a) The waveform of the primary current and the output voltage of the inverter in fundamental wave channel; (b) The waveform of the primary current and the output voltage of the inverter in harmonic channel; (c) The waveform of the primary current of fundamental wave channel and the harmonic channel; (d) The waveform of the secondary-side network current

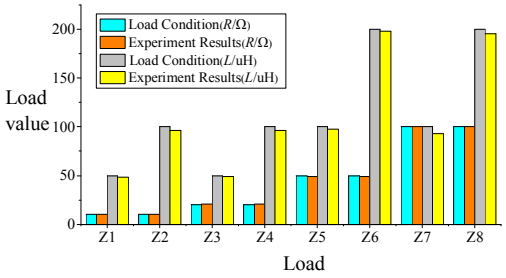

Fig. 10. Experiment results of the load identification

side current waveform with superposition of the fundamental wave current and the third harmonic current.

In order to verify the identification effect of this algorithm, many groups of comparison between actual load values and the experiment results have been presented in Table 4 and Fig. 10. From it, the technology proposed to achieve the load identification of ICPT system utilizing harmonics not only has high accuracy, but also can work under normal power transmission. Furthermore, according to analysis of the system characteristics, constant voltage characteristics of the system secondary-side network will lead to efficiency decrease under the light loads.

7. Conclusion

First, this paper states the working principle and mode of the ICPT system for load identification utilizing harmonics. Second, a fundamental-harmonic double channel system is established, and the fundamental wave current and the third harmonic current can be achieved by Fourier decomposition in the secondary-side network when load identification is needed, and then get the resistance-inductive load parameters; Finally, the experiment indicates that the technology proposed can accurately tracks the load vibration. From the former theoretical analysis, it can be concluded that the system efficiency would be higher under heavy load condition, lower under light load condition. However, there is the cross coupling in the magnetic circuit structure, and the deviations in the parameters selection and measurement have influence on identification accuracy, further research will be done to take these factors into consideration.

Acknowledgments

This work was supported by the National Natural Science Foundation of China (Grant No. 51777210) and the Jiangsu Natural Science Foundation (Grant No. BK20171190).

References

[1] H. H. Wu, G. A. Covic, J. T. Boys and D. J. Robertson, "A Series-Tuned Inductive-Power-Transfer Pickup with a Controllable AC-Voltage Output," *IEEE Transactions on Power Electronics*, vol. 26, no. 1, pp. 98-109, Jan. 2011.

[2] H. Matsumoto, Y. Neba, K. Ishizaka and R. Itoh, "Comparison of Characteristics on Planar Contactless Power Transfer Systems," *IEEE Transactions on Power Electronics*, vol. 27, no. 6, pp. 2980-2993, June 2012.

[3] M.J. Neath, U.K. Madawala and D.J. Thrimawithana, "A new controller for bi-directional inductive power transfer systems," *IEEE International Symposium on Industrial Electronics, Gdansk*, pp. 1951-1956, 2011

[4] Y. Liu, R. Mai, P. Yue and Z. He, "A dynamic tuning method utilizing inductor paralleled with load for inductive power transfer," *IEEE Applied Power Electronics Conference and Exposition* (*APEC*)*, San Antonio*, pp. 1076-1079, 2018.

[5] C. S. Tang, Y. Sun, Y. G. Su, S. K. Nguang and A. P. Hu, "Determining Multiple Steady-State ZCS Operating Points of a Switch-Mode Contactless Power Transfer System," *IEEE Transactions on Power Electronics*, vol. 24, no. 2, pp. 416-425, Feb. 2009.

[6] M. Budhia, G. A. Covic and J. T. Boys, "Design and Optimization of Circular Magnetic Structures for Lumped Inductive Power Transfer Systems," *IEEE Transactions on Power Electronics*, vol. 26, no. 11, pp. 3096-3108, Nov. 2011.

[7] Su Y., Chen L and Wang Z, "A load identification method for inductive power transfer system based on the least squares algorithm," *Transactions of China Electrotechnical Society*, 2015, 30, (5), pp. 9-14.

[8] Z. H. Wang, Y. P. Li, Y. Sun, C. S. Tang and X. Lv, "Load Detection Model of Voltage-Fed Inductive Power Transfer System," *IEEE Transactions on Power Electronics*, vol. 28, no. 11, pp. 5233-5243, Nov. 2013.

[9] M. Khalilian, S. G. Rosu, V. Cirimele, P. Guglielmi and R. Ruffo, "Load identification in dynamic wireless power transfer system utilizing current injection in the transmitting coil," *IEEE Wireless Power Transfer Conference* (*WPTC*)*,* Aveiro, 2016, pp. 1-4.

[10] G. R. Nagendra, L. Chen, G. A. Covic and J. T. Boys, "Detection of EVs on IPT highways," *IEEE Applied Power Electronics Conference and Exposition - APEC*, 2014, pp. 1604-1611.

[11] D. Lin, J. Yin and S. Y. R. Hui, "Parameter identification of wireless power transfer systems using input voltage and current," *IEEE Energy Conversion Congress and Exposition* (*ECCE*), PA, pp. 832-836, 2014.

[12] Hu Si deng and Liang Zi peng, "Research of the contactless load detection based on characteristic parameters in transient process," *Proceedings of the CSEE*, 2017, 37, (6), pp. 1850-1856.

[13] Dai X, Sun Y and Su Y G, "Study on constant current control of inductive power transfer with parameter identification," *Journal of Chongqing University*, 2011, 34, (6), pp. 98-104.

[14] Yue S, Wei H and Yu Gang Su, "A load identification algorithm for contactless power transmission systems," *Journal of Chongqing University*, 2009, 32, (2), pp. 141-145.

[15] A. Dominguez, A. Otin, I. Urriza, L. A. Barragan, D. Navarro and J. I. Artigas, "Load identification of

domestic induction heating based on Particle Swarm Optimization," *IEEE 15th Workshop on Control and Modeling for Power Electronics* (*COMPEL*), 2014, pp. 1-6.
[16] D. Navarro, Ó. Lucı´a, L. A. Barragán, I. Urriza and Ó. Jiménez, "High-Level Synthesis for Accelerating the FPGA Implementation of Computationally Demanding Control Algorithms for Power Converters," *IEEE Transactions on Industrial Informatics*, vol. 9, no. 3, pp. 1371-1379, Aug. 2013.
[17] Xia C Y, Ren S Y and Nian M, "Inductively Coupled Power Transfer System with Fundamental Wave and Harmonic Wave Two-path Parallel Transmission," *Automation of Electric Power Systems*, 2017.
[18] Zou A, Wang H and Hua J, "The movable ICPT system with multi-loads based on the LCL compensation circuit," *Transactions of China Electrotechnical Society*, 2014, 34, (24), pp. 4000-4006.
[19] J Li, C Liao and L Wang, "Decoupling method of maximum efficiency and transferring power for electric vehicle wireless charging system via LCCL circuit," *Transactions of China Electrotechnical Society*, 2015, 30, (s1), pp. 199.

Chen-Yang Xia He received the B.S., M.S., and Ph.D. degrees in control theory and control engineering from Chongqing University, Chongqing, China, in 2006, 2008, and 2010, respectively. He is currently an Associate Professor in the School of Electrical & Power Engineering, China University of Mining and Technology, Xuzhou, China. His current research interests include intrinsic safety switch power supply and wireless power transfer.

Wen-Ting Zhu She was born in AnHui Province, China, in 1993. She received the B.S. degree in electrical engineering from China University of Mining and Technology, Xuzhou, China, in 2016. She is currently working towards his M.S. degree in the School of Electrical & Power Engineering, China University of Mining and Technology. Her current research interests include wireless power transfer.

Nian Ma He was born in HeNan Province, China, in 1993. He received the B.S. degree in electrical engineering from China University of Mining and Technology, Xuzhou, China, in 2016. He is currently working towards his M.S. degree in the School of Electrical & Power Engineering, China University of Mining and Technology. His current research interests include wireless power transfer.

Ren-Hai Jia He was born in AnHui Province, China, in 1993. He received the B.S. degree in electrical engineering from China University of Mining and Technology, Xuzhou, China, in 2017. He is currently working towards his M.S. degree in the School of Electrical & Power Engineering, China University of Mining and Technology. His current research interests include wireless power transfer.

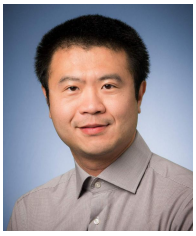

Qiang Yu He received his bachelor's degree in Northwestern Polytechnical University in 2008, and obtained his doctorate in Social Psychology Munich University of the Federal Armed Forces in 2012.; Awarded the outstanding staff award of Munich federal Defense Force University, the European Commission Marie Curie prize, published more than 30 SCI/EI papers, published two monographs. His current research interests motor design, motor control and power electronics.